THE JOURNAL OF PHYSICAL CHEMISTRY B
A JOURNAL OF THE AMERICAN CHEMICAL SOCIETY

pubs.acs.org/JPCB

Article

Fluorescent H-Aggregate Vesicles and Tubes of a Cyanine Dye and Their Potential as Light-Harvesting Antennae

Nitin Ramesh Reddy, Megan Aubin, Akihiro Kushima, and Jiyu Fang*

Cite This: *J. Phys. Chem. B* 2021, 125, 7911−7918

Read Online

ACCESS | Metrics & More | Article Recommendations | SI Supporting Information

ABSTRACT: H-aggregates of π-conjugated dyes are an ordered supramolecular structure. However, the non-fluorescence behavior of H-aggregates greatly limits their potential applications. In this paper, we report the formation of fluorescent H-aggregates with vesicular and tubular morphologies by the self-assembly of 3,3′-diethylthiacarbocyanine iodide ($DiSC_2(3)$) in ammonia/methanol mixtures. The transition from H-aggregate vesicles to H-aggregate tubes can be achieved by increasing the volume fraction of methanol in the mixtures. H-aggregate vesicles and tubes show two blue-shifted absorption bands and strong fluorescence, which result from the inclined arrangement of $DiSC_2(3)$ molecules. Furthermore, light-harvesting complexes are formed by adding dopamine (DA)-quinone (acceptor) in synthetic urine with H-aggregate vesicles or tubes. Our results show that H-aggregate tubes are more efficient than H-aggregate vesicles in transferring excited electrons to DA-quinone acceptors.

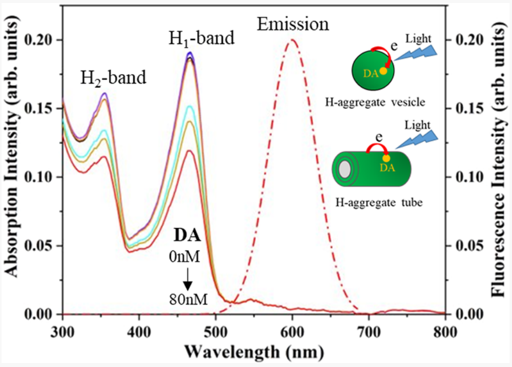

1. INTRODUCTION

Ordered aggregates of π-conjugated dyes are a potential candidate for fabricating sensitized solar cells, mimicking light-harvesting photosynthetic antennae and designing optical probes because their optical and excitonic properties significantly differ from those of individual dyes.[1,2] H-aggregates of π-conjugated dyes represent an ordered supramolecular structure, in which the transition dipole moments of π-conjugated dyes are in a face-to-face arrangement. It has been shown that H-aggregates of π-conjugated dyes can effectively contribute to the photocurrent in photovoltaic cells[3] and have high optical coefficients for nonlinear optics.[4] Based on the exciton theory, the coupling of the transition dipole moments of π-conjugated dyes leads to the formation of two energy exciton states, in which optical transitions to the higher-energy exciton state are only allowed for the face-to-face arrangement of H-aggregates. Due to the rapid relaxation of the excited energy from the higher-energy exciton state to the lower-energy exciton state (forbidden), H-aggregates usually exhibit no fluorescence emission.[5] Although the non-fluorescence behavior is a common feature of H-aggregates, several cases of fluorescent H-aggregates are reported in the literature.[6−13] It is generally believed that the fluorescence from H-aggregates is mainly due to the imperfect face-to-face arrangement of π-conjugated dyes, in which fluorescence arising from the lower-energy exciton state becomes possible.[14]

Cyanine dyes are ionic organic compounds that consist of two heterocyclic units connected by a polymethine chain.[15] Like many other self-assembly systems, electrostatic, hydrophobic, and van der Waals interactions play important roles in the aggregation of ionic cyanine dyes. The balance of these interactions determines the extent and type of aggregation of cyanine dyes. There has been great interest in controlling the aggregation of cyanine dyes in solution by manipulating these interactions.[16−27] In this paper, we studied the aggregation behavior of 3,3′-diethylthiacarbocyanine iodide ($DiSC_2(3)$) in ammonia/methanol mixtures. Especially, we found that $DiSC_2(3)$ formed fluorescent H-aggregates, which changed their morphologies from vesicles to tubes with the increase in the volume fraction of methanol in the mixtures. The H-aggregate vesicles and tubes showed two blue-shifted H-bands and strong fluorescence emission. The inclined arrangement of $DiSC_2(3)$ molecules in H-aggregate vesicles and tubes was evident from their absorption spectra, which was considered responsible for the origin of fluorescence. In comparison with J-aggregates, the application of H-aggregates as light-harvesting antennae is still limited. We formed light-harvesting complexes by adding dopamine (DA)-quinone (acceptor) in synthetic urine with H-aggregate vesicles and tubes to understand whether the H-aggregates could be beneficial for the transfer of excited electrons to DA-quinone acceptors.

Received: May 13, 2021
Revised: June 10, 2021
Published: July 7, 2021

ACS Publications

https://doi.org/10.1021/acs.jpcb.1c04262

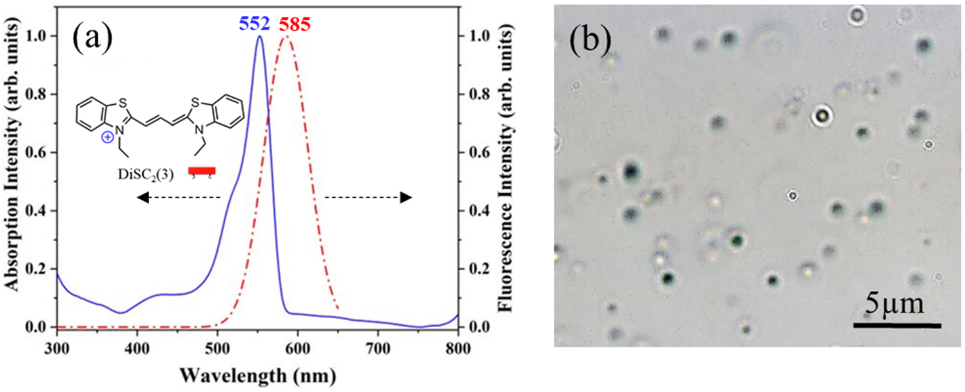

Figure 1. (a) Absorption and fluorescence spectra of 1 mM DiSC$_2$(3) in 7% ammonia solution after being aged for 1 week at room temperature. (b) Optical microscopy image of spherical aggregates of DiSC$_2$(3) formed in 7% ammonia solution after being aged for 1 week. The chemical structure of DiSC$_2$(3) was inserted in panel (a).

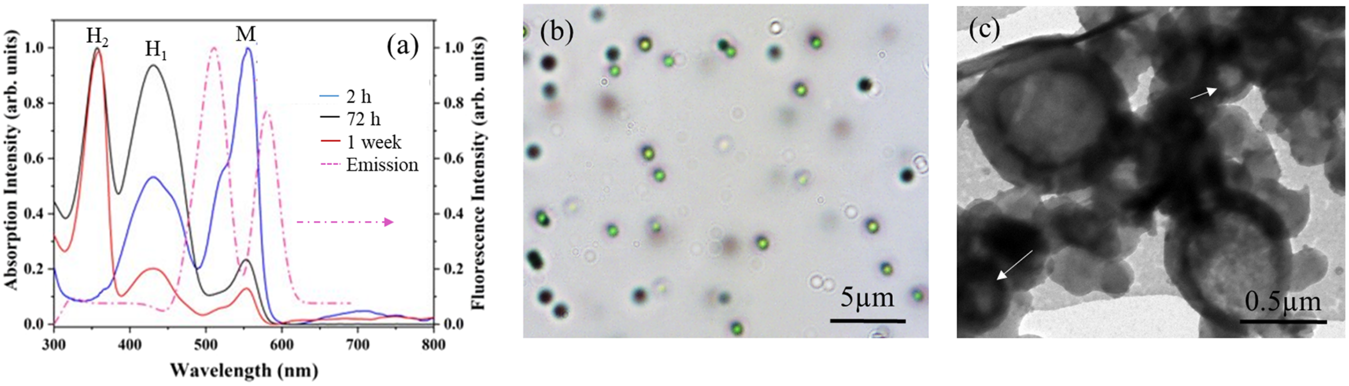

Figure 2. (a) Absorption spectra of 1 mM DiSC$_2$(3) in 30% ammonia solution after being aged for different periods of time at room temperature. Optical microscopy (b) and TEM (c) images of H-aggregate vesicles formed in 30% ammonia solution after being aged for 1 week. The fluorescence spectrum of 1 mM DiSC$_2$(3) in 30% ammonia solution after being aged for 1 week was inserted in panel (a). The monomer band was denoted as M.

2. EXPERIMENTAL SECTION

2.1. Materials. 3,3′-Diethylthiacarbocyanine iodide (DiSC$_2$(3)) and dopamine (DA) were purchased from Sigma-Aldrich and used without purification. Deionized (DI) water (18 MΩ cm, pH 5.7) was obtained from an Easypure II system. Methanol and ammonia solution were from Sigma-Aldrich. Synthetic urine with pH 7.8−8.0 was purchased from the Ricca Chemical Company and diluted 10 times with DI water before being used. Holey Formvar filmed grids were from Electron Microscopy Science.

2.2. Formation of H-Aggregates. For the formation of H-aggregate vesicles, DiSC$_2$(3) was dissolved in ammonia solution. Meanwhile, for the formation of H-aggregate tubes, DiSC$_2$(3) was dissolved in methanol and then mixed with ammonia solution. These mixed solutions were sonicated at ∼50 °C in an ultrasonic bath (Branson 1510, Branson Ultrasonics Co.) for 5 min and then allowed to sit in the dark at room temperature. Over time, these mixed solutions changed color, suggesting the H-aggregation of DiSC$_2$(3). These H-aggregate solutions of DiSC$_2$(3) were stored in the dark when they were not in use.

2.3. Characterizations. The structure and morphology of H-aggregates were characterized with an optical microscope (Olympus BX), a fluorescence microscope (Cytation 5 imaging reader) equipped with a Xenon flash lamp and a DAPI filter cube, and a transmission electron microscope (FEI Techni F30). For optical microscope observations, a drop of H-aggregate solution was placed on a glass substrate followed by placing a cover glass slide on top of the drop. For transmission electron microscopy (TEM) measurements, a drop of H-aggregate solution was dried on holey Formvar filmed grids at room temperature for 24 h and then imaged at an accelerating voltage of 300 kV. Dynamic light scattering was performed with PD 2000DLS. For spectroscopy studies, H-aggregate solution was added to a cuvette. The absorption and fluorescence emission spectra were taken with a Cary 60 spectrophotometer and a Jasco FP-6500 spectrofluorometer, respectively.

2.4. Formation of H-Aggregate-Integrated Agarose Films. Agarose solution (1 wt %) was formed by dissolving 0.1 g of agarose powder in 10 mL of 1% ammonia solution at ∼40 °C under magnetic stirring. H-aggregate tube solution (2.5 mL) was then mixed with 2.5 mL of agarose solution. The mixed solution was stirred for 2 min and then transferred onto a horizontally placed quartz cuvette on a table. H-aggregate tube-integrated agarose hydrogel films were formed on the wall of the quartz cuvette when the temperature was cooled to 23 °C.

3. RESULTS AND DISCUSSION

DiSC$_2$(3) consists of a π-conjugated polymethine backbone and two short alkyl tails bearing three carbons (see the inset in

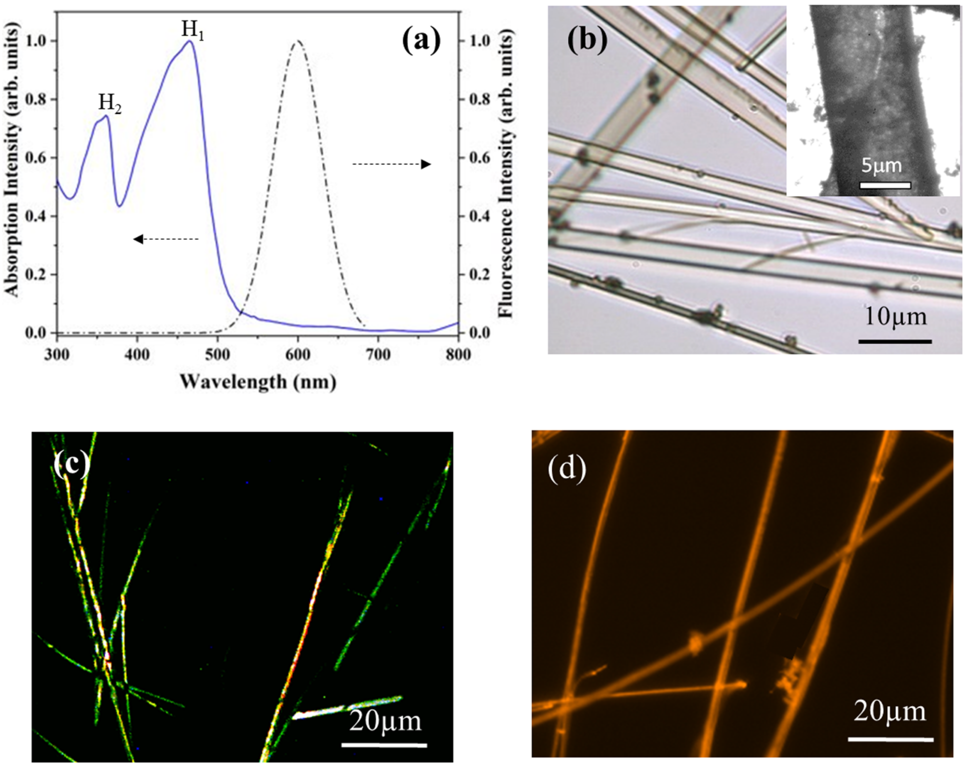

Figure 3. (a) Absorption and fluorescence spectra of 1 mM DiSC$_2$(3) in the methanol/ammonia mixture (1:1, v/v) after being aged for 1 week at room temperature. (b) Optical, (c) polarizing, and (d) florescence microscopy images of H-aggregate tubes of DiSC$_2$(3) formed in the methanol/ammonia mixture (1:1, v/v) after being aged for 1 week. The TEM image of H-aggregate tubes was inserted in panel (b).

Figure 1a). DiSC$_2$(3) (1 mM) in 7% ammonia solution showed an absorption band at 552 nm and an emission band at 585 nm after being aged for 72 h at room temperature (Figure 1a). The absorption band was identical to the monomer band reported in the literature.[27] Optical microscopy images revealed that 1 mM DiSC$_2$(3) formed spherical aggregates in 7% ammonia solution (Figure 1b). Based on the spectroscopy and microscopy results, we concluded that DiSC$_2$(3) molecules formed a disordered structure in the spherical aggregates.

When the concentration of ammonia was increased to 30%, 1 mM DiSC$_2$(3) showed a monomer band at 552 nm and a blue-shifted band at 431 nm after being aged for 2 h at room temperature (Figure 2a). The blue-shifted band was denoted as the H$_1$-band. After the solution was aged for 72 h, the intensity of the monomer band significantly decreased, while the intensity of the H$_1$-band increased. At the same time, another blue-shifted band appeared at 358 nm, which was denoted as the H$_2$-band. After 1 week of aging, the H$_2$-band becomes dominant (Figure 2a). There was no further change in the absorption spectra for longer aging. According to the exciton theory, H-aggregates of dyes strongly quench their fluorescence if dyes are stacked in the perfect face-to-face arrangement. However, the H-aggregates of DiSC$_2$(3) formed in 30% ammonia solution showed an emission band at 580 nm with a Stokes shift of 28 nm with respect to the monomer band and an emission at 510 nm with a large Stokes shift of 79 nm with respect to the H$_1$-band (Figure 2a). The large Stokes shift is a character of fluorescent H-aggregates. The H-aggregates showed spherical morphology (Figure 2b). TEM analysis revealed that the spherical H-aggregates were polydispersed with the diameter in the range from 0.1 to 0.7 μm (Figure 2c). The hollowness was visible from large spherical H-aggregates, suggesting that DiSC$_2$(3) formed vesicular-like H-aggregates. The wall thickness of large H-aggregate vesicles was ~150 nm. Although the majority of small spherical H-aggregates shown in the TEM image appeared to be flat, the hollow spherical H-aggregates were occasionally observed, as indicated by the arrows in Figure 2c. The flattening of small spherical H-aggregates was likely caused by the drying process on substrates. Dynamic light scatting revealed that the average diameter of small spherical H-aggregates was ~0.22 μm (Figure S1).

The aggregation of DiSC$_2$(3) molecules in ammonia solution was likely driven by $\pi-\pi$ stacking, electrostatic, and hydrophobic interactions. Ammonia is a weak base and converts to ammonium ions (NH_4^+) and hydroxide ions (OH^-) by the deprotonation of water. The observed monomer band in 7% ammonia solution might suggest that the electrostatic repulsion of positively charged DiSC$_2$(3) molecules prevented them to form an ordered structure in aggregate vesicles. With the increase in ammonia concentrations, the concentration of OH^- ions increased. The increased OH^- concentrations might fully screen the charge of DiSC$_2$(3) molecules and reduced the electrostatic repulsion between them, consequently leading to the formation of H-aggregates in the wall of vesicles.

Furthermore, we studied the aggregation behavior of DiSC$_2$(3) in methanol/ammonia mixtures. In our experiments, DiSC$_2$(3) was dissolved in methanol and then mixed with 30% ammonia solution. After being aged for 1 week at room temperature, 1 mM DiSC$_2$(3) in the methanol/ammonia mixture (1:9, v/v) showed a strong H$_2$-band at 358 nm and a weak H$_1$-band at 416 nm (Figure S2a). The H-aggregates

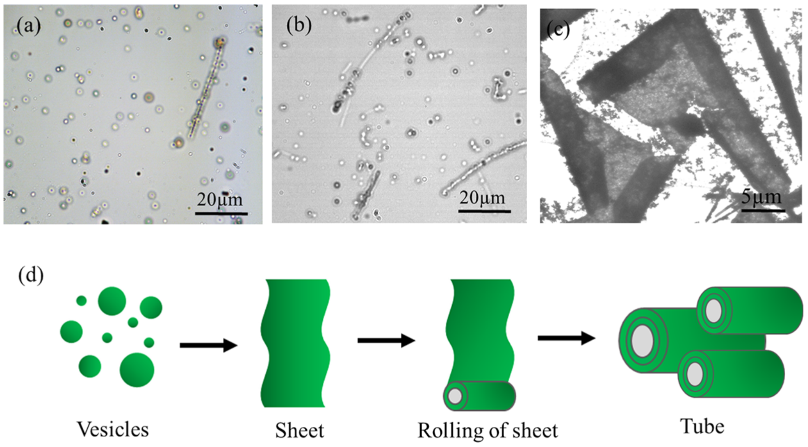

Figure 4. Optical microscopy images of H-aggregate vesicles of 1 mM $DiSC_2(3)$ in the methanol/ammonia mixture (1:1, v/v) after being aged for 24 h (a) and 48 h (b) at room temperature. (c) TEM image of H-aggregate tubes formed by 1 mM $DiSC_2(3)$ in the methanol/ammonia mixture (1:1, v/v). (d) Schematic illustration of the possible formation mechanism of H-aggregate tubes from H-aggregate vesicles.

showed spherical morphology (Figure S2b), which was similar to the H-aggregates formed in 30% ammonia solution. In the methanol/ammonia mixture (1:1, v/v), 1 mM $DiSC_2(3)$ showed a weak H_2-band at 361 nm and a strong H_1-band at 465 nm (Figure 3a) after being aged for 1 week. In this case, the monomer band completely disappeared. The H-aggregates showed a strong fluorescence emission at 600 nm with a large Stokes shift of 135 nm with respect to the strong H_1-band (Figure 3a). Optical microscopy images revealed that the H-aggregates had tubular morphology with the optical contrast between the tube walls and the inner channel (Figure 3b), in which the inner channel appeared light, while the tube walls appeared as two parallel dark lines. The external diameter of H-aggregate tubes was in the range of 2−6 μm. The hollowness of H-aggregate tubes was visible in a TEM image, although the contrast difference between the tube walls and the inner channel was small (see the inset in Figure 3b). When being viewed between two crossed polarizers, the H-aggregate tubes showed birefringence (Figure 3c), suggesting that they had a long-range crystalline structure. Figure 3d shows the fluorescence microscopy image of H-aggregate tubes, which revealed that they were highly fluorescent. H-aggregate tubes showing two H-bands in absorption spectra could also be formed by 0.5 and 2.0 mM $DiSC_2(3)$ in the methanol/ammonia mixture (1:1, v/v) (Figure S3). The diameter of the H-aggregate tubes formed by 2.0 mM $DiSC_2(3)$ was larger than that by 0.5 mM $DiSC_2(3)$. In addition, some of the H-aggregate tubes formed by 0.5 mM $DiSC_2(3)$ appeared to be curved.

To gain a better understanding of the formation mechanism of H-aggregate tubes, we imaged the aggregates of $DiSC_2(3)$ formed at early stages. After 2 h of aging, the vesicular aggregates of $DiSC_2(3)$ were observed (Figure 4a). The vesicles then linear-aggregated over time (Figure 4b). TEM images revealed that H-aggregate tubes coexisted with partially rolled sheets (Figure 4c). The presence of partially rolled sheets strongly suggested that H-aggregate tubes were formed by the rolling up of a sheet. Thus, a possible formation mechanism of the H-aggregate tubes is illustrated in Figure 4d. First, the fusion of linearly aggregated vesicles formed flat sheets, which likely resulted from the crystallization of $DiSC_2(3)$. The crystalline sheets then rolled up into H-aggregate tubes, which was similar to the formation of tubes from the self-assembly of chiral bile acids.[28] The formation of tubes starting from the vesicles of a chiral bile salt-derived molecule was also reported.[29] The chiral interaction was proposed to be a driving force for the formation of tubular structures from chiral membranes, in which chiral molecules are twisted with respect to each other.[30] However, $DiSC_2(3)$ is an achiral molecule. The rolling up of $DiSC_2(3)$ sheets cannot be explained with the chiral interaction. The birefringence domains are observed in Figure 3c. Thus, the presence of different crystalline domains in $DiSC_2(3)$ sheets may be the origin of the rolling up of $DiSC_2(3)$ sheets.[31]

The appearance of two blue-shifted H-bands in absorption spectra (referred as Davydov splitting[14]) suggested the inclined arrangement of $DiSC_2(3)$ molecules in H-aggregate vesicles and tubes. There were differences in the absorption spectra between H-aggregate tubes and H-aggregate vesicles after 1 week of aging (Figures 2a and 3a). Although the H_2-band position of H-aggregate tubes was near the same as that of H-aggregate vesicles, the H_1-band position of H-aggregate tubes was less blue-shifted than that of H-aggregate vesicles. Furthermore, the H-aggregate tubes showed the predominance of the H_1-band over the H_2-band, while the H-aggregate vesicles showed the predominance of the H_2-band over the H_1-band. The inclination angle (θ) of $DiSC_2(3)$ molecules in H-aggregate vesicles and tubes could be calculated from the oscillation strength of the two Davydov components (H_1- and H_2-bands) with the equation[32,33] $\tan^2\frac{\theta}{2} = \frac{A_{\text{H1-band}}}{A_{\text{H2-band}}}$, where $A_{\text{H1 - band}}$ and $A_{\text{H2 - band}}$ are the oscillation strengths of the H_1-band and the H_2-band, respectively. The ratio of $A_{\text{H1 - band}}/A_{\text{H2 - band}}$ is proportional to the ratio of the areas under the H_1-band and the H_2-band in adsorption spectra. However, the overlap of the H_1-band and the H_2-band limited the possibility of measuring the area under the H_1-band and the H_2-band. Thus, we used the intensity ratio of the H_1-band and the H_2-band to replace the area ratio under them to roughly estimate the inclined angles (θ) of $DiSC_2(3)$ molecules to be ~48° in H-aggregate vesicles and ~97° in H-aggregate tubes.

From the results, we concluded that the inclined arrangement of $DiSC_2(3)$ molecules was the origin of the fluorescence from H-aggregate vesicles and tubes. Figure 5 illustrates the energy band diagram and optical transitions of H-aggregate vesicles and tubes, in which $DiSC_2(3)$ molecules form the

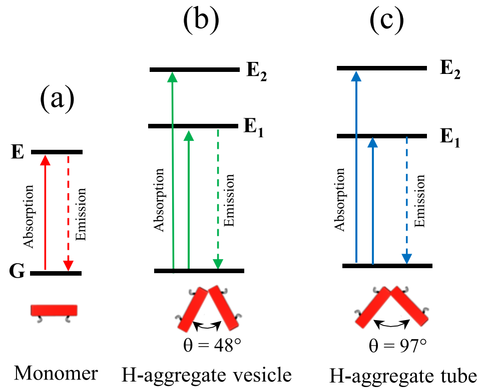

Figure 5. Schematic energy diagram and optical transition of monomers (a), H-aggregate vesicles (b), and H-aggregate tubes (c). Schematic illustrations for the inclined arrangement of $DiSC_2(3)$ molecules in H-aggregate vesicles and tubes were inserted in panels (b, c), respectively. θ was the inclined angle.

inclined arrangements. The coupling of $DiSC_2(3)$ molecules in H-aggregate vesicles and tubes led to the formation of two energy excited states (E_1 and E_2). Due to the inclined arrangement of $DiSC_2(3)$ molecules in H-aggregate vesicles and tubes, the optical transitions from the ground state (E) to E_1 and E_2 gave two blue-shifted H-bands. The excitation of H-aggregate vesicles and tubes rapidly relaxed from the E_2 to E_1 states by nonradiative internal conversion. The red-shifted fluorescence emission increased from the E_1 state. The observed large Stokes shift of fluorescence emissions was a characteristic property of H-aggregates.

It was reported that H-aggregates of thionine dyes could harvest light energy and then transfer energy to the monomeric dye.[34] Dopamine (DA) is a neurotransmitter, which carries signals between neurons. The oxidized DA (DA-quinone) could serve as an electron acceptor.[35,36] A previous study showed that DA could be oxidized in synthetic urine with pH 7.8−8.0.[37] Thus, we formed light-harvesting complexes by adding DA in synthetic urine with disordered aggregate vesicles and H-aggregate vesicles. Figure 6a shows the absorption spectra of spherical aggregates (Figure 1b) in diluted synthetic urine (100 times) with DA. We found that the absorption band at 552 nm (monomer band) only showed slight variations after the addition of DA. However, the H_2-band intensity of H-aggregate vesicles gradually decreased with the increase in DA concentrations from 10 to 80 nM (Figure 6b). The plot of the relative intensity ($\Delta I/I_0$) of the H_2-band as a function of DA concentrations showed a linear relationship (see the inset in Figure 6b). Here, $\Delta I = I_0 - I$, where I_0 is the H_2-band intensity before the addition of DA and I is the H_2-band intensity after the addition of DA.

We noted that the H-aggregate tubes of $DiSC_2(3)$ slowly precipitated in solution over time. Thus, we integrated them in transparent and neutral agarose hydrogel films, which were permeable for small molecules.[38,39] Figure 7a shows the photography image of the H-aggregate tube-integrated agarose hydrogel film formed on the wall of a cuvette. After the addition of 1 mL of diluted synthetic urine, the intensities of both the H_1-band and H_2-band of the integrated H-aggregate tubes increased over time and then leveled off after 2 h (Figure S4). The increased intensities of the H_1-band and H_2-band were the result of the shrinkage of the agarose hydrogel films (Figure S5), which led to the increase in the density of H-aggregate tubes in the hydrogel film. Thus, we recorded the absorption spectra 2 h after the addition of diluted synthetic urine with DA, in which the shrinkage of the hydrogel film was stopped. In this case, the integrated H-aggregate tubes showed no change in their absorbance in diluted synthetic urine with/without light irradiation (Figure S6). However, the decrease in the H-band intensity of the integrated H-aggregate tubes was observed after the addition of DA (Figure 7b). The $\Delta I/I_0$ of the H_1-band and H_2-band linearly increased with the increase in DA concentrations (Figure 7c and Figure 7d, respectively).

In the light-harvesting system, the oxidized DA (DA-quinone) in synthetic urine likely adsorbed on the surface of H-aggregate vesicles and tubes through the $\pi-\pi$ stacking interaction. The gradual decrease in the absorbance of H-aggregate vesicles and tubes with the increase in DA concentrations might result from either electron or energy transfer to DA-quinone acceptors. DA-quinone had an absorption band at 280 nm,[37,39] which did not overlap with the fluorescence band of H-aggregate vesicles (510 nm) and tubes (600 nm). The energy transfer from H-aggregate vesicles and tubes to DA-quinone acceptors could be excluded. Therefore, we concluded that the electron transfer from the excited H-aggregate vesicles and tubes to DA-quinone acceptors was responsible for the decrease in their absorbance. Our results showed that the absorbance of spherical aggregates (Figure 1b) basically remained unchanged (Figure 6a),

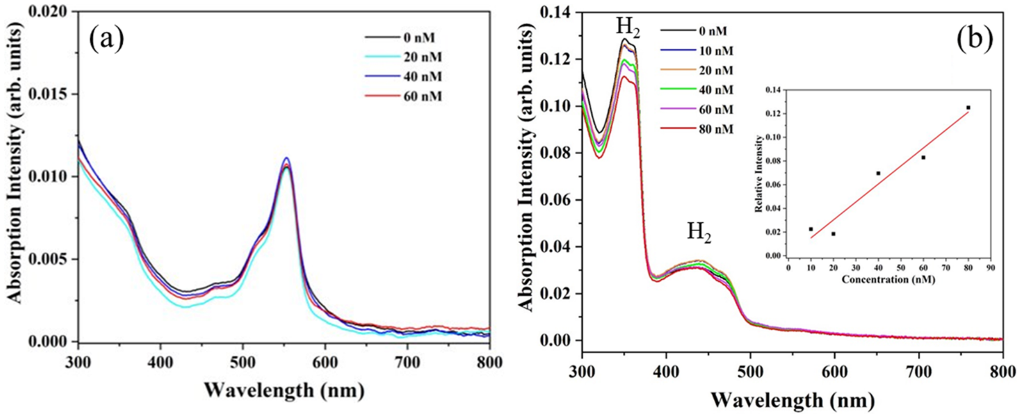

Figure 6. Absorption spectra of spherical aggregates (a) and H-aggregate vesicles (b) in synthetic urine with DA at different concentrations. The plot of the relative intensity ($\Delta I/I_0$) of the H_2-band as a function of DA concentrations was inserted in panel (b).

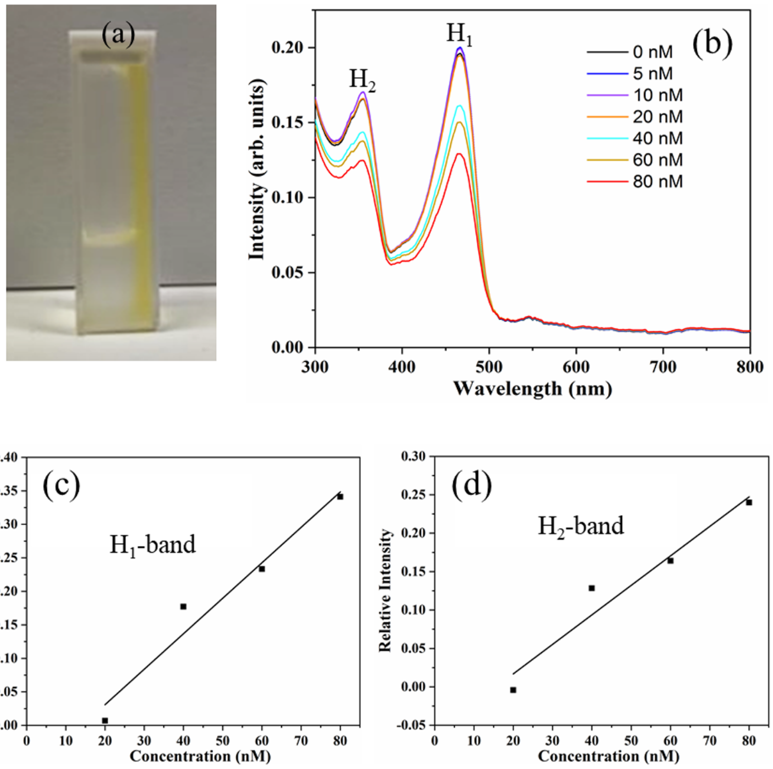

Figure 7. (a) Photography image of the H-aggregate tube-integrated hydrogel film formed on the wall of a quartz cuvette filled by synthetic urine with DA. (b) Absorption spectra of H-aggregate tube-integrated agarose hydrogel films taken 2 h after the addition of synthetic urine with 0, 10, 20, 40, 60, and 80 nM DA. Plots of the relative intensity ($\Delta I/I_0$) of the H$_1$-band (c) and the H$_2$-band (d) as a function of DA concentrations.

suggesting that they were unable to efficiently transfer the excited electrons to DA-quinone acceptors. It was likely that the delocalized excitons of H-aggregate vesicles and tubes felicitated the transfer of excited electrons to DA-quinone acceptors. In addition, H-aggregate vesicles only showed in the gradual decrease in the H$_1$-band with the increase in DA concentrations (Figure 6b). For H-aggregate tubes, both the H$_1$- and H$_2$-bands gradually decreased with the increase in DA concentrations (Figure 7b). Furthermore, the slope of the plot of the $\Delta I/I_0$ of H$_1$- and H$_2$-bands of H-aggregate tubes as a function of DA concentrations was larger than that of the H$_1$-band of H-aggregate vesicles. These results suggested that H-aggregate tubes were more efficient than H-aggregate vesicles for transferring excited electrons to DA-quinone acceptors. As can be seen in Figures 6b and 7b, the H-bands of H-aggregate tubes were sharper than those of H-aggregate vesicles, suggesting that the coupling of DiSC$_2$(3) molecules in H-aggregate tubes was stronger than that of H-aggregate vesicles. This might explain why H-aggregate tubes were more favorable for the transfer of excited electrons to DA-quinone acceptors, compared to H-aggregate vesicles.

4. CONCLUSIONS

We show that DiSC$_2$(3) molecules can form fluorescent H-aggregate vesicles and tubes in ammonia/methanol mixtures. In particular, the transition from H-aggregate vesicles to H-aggregate tubes can be achieved by increasing the volume ratio of methanol in the mixtures. The H-aggregate vesicles and tubes show two H-bands in the absorption spectra, referred as Davydov splitting. The inclined angle of DiSC$_2$(3) molecules in H-aggregate vesicles and tubes is estimated from their absorption spectra. The fluorescence from H-aggregate vesicles and tubes results from the inclined arrangement of DiSC$_2$(3) molecules. Light-harvesting complexes are formed by adding DA in synthetic urine with H-aggregate vesicles or tubes. Our results show that H-aggregate tubes are more efficient than H-aggregate vesicles in transferring excited electrons to DA-quinone acceptors.

■ ASSOCIATED CONTENT

Supporting Information

The Supporting Information is available free of charge at https://pubs.acs.org/doi/10.1021/acs.jpcb.1c04262.

Adsorption spectra of H-aggregate vesicles and tubes, optical microscopy images of H-aggregate vesicles and tubes, and photographic images of agarose hydrogels (PDF)

■ AUTHOR INFORMATION

Corresponding Author

Jiyu Fang − *Department of Materials Science and Engineering and Advanced Materials Processing and Analysis Center, University of Central Florida, Orlando, Florida 32816, United States;* orcid.org/0000-0002-6056-5113; Email: Jiyu.Fang@ucf.edu

Authors

Nitin Ramesh Reddy − *Department of Materials Science and Engineering and Advanced Materials Processing and Analysis Center, University of Central Florida, Orlando, Florida 32816, United States;* orcid.org/0000-0002-5168-0507

Megan Aubin − *Department of Materials Science and Engineering and Advanced Materials Processing and Analysis*

Center, University of Central Florida, Orlando, Florida 32816, United States

Akihiro Kushima – *Department of Materials Science and Engineering and Advanced Materials Processing and Analysis Center, University of Central Florida, Orlando, Florida 32816, United States;* orcid.org/0000-0001-5166-4198

Complete contact information is available at:
https://pubs.acs.org/10.1021/acs.jpcb.1c04262

Notes

The authors declare no competing financial interest.

■ ACKNOWLEDGMENTS

This work was supported by the U.S. National Science Foundation (CBET 1803690).

■ REFERENCES

(1) Würthner, F.; Kaiser, T. E.; Saha-Möller, C. R. J-aggregates: From Serendipitous Discovery to Supramolecular Engineering of Functional Dye Materials. *Angew. Chem., Int. Ed.* **2011**, *50*, 3376–3410.

(2) Elemans, J. A. A. W.; van Hameren, R.; Nolte, R. J. M.; Rowan, A. E. Molecular Materials by Self-Assembly of Porphyrins, Phthalocyanines, and Perylenes. *Adv. Mater.* **2006**, *18*, 1251–1266.

(3) Nasr, C.; Liu, D.; Hotchandani, S.; Kamat, P. V. Dye-Capped Semiconductor Nanoclusters. Excited State and Photosensitization Aspects of Rhodamine 6G H-aggregates Bound to SiO_2 and SnO_2 Colloids. *J. Phys. Chem.* **1996**, *100*, 11054–11061.

(4) Xu, Z.; Lu, W.; Bohn, P. W. Electronic Resonance and Local Field Effects on the Nonlinear Optical Activity of H-Aggregate-Forming Stilbazolium Amphiphiles. *J. Phys. Chem.* **1995**, *99*, 7154–7159.

(5) Spano, F. C. The Spectral Signatures of Frenkel Polarons in H- and J-Aggregates. *Acc. Chem. Res.* **2010**, *43*, 429–439.

(6) Peyratout, C.; Daehne, L. Aggregation of Thiacyanine Derivatives on Polyelectrolytes. *Phys. Chem. Chem. Phys.* **2002**, *4*, 3032–3039.

(7) Rösch, U.; Yao, S.; Wortmann, R.; Würthner, F. Fluorescent H-Aggregates of Merocyanine Dyes. *Angew. Chem., Int. Ed.* **2006**, *45*, 7026–7030.

(8) Fang, Q.; Wang, F.; Zhao, H.; Liu, X.; Tu, R.; Wang, D.; Zhang, Z. Strongly Coupled Excitonic States in H-Aggregated Single Crystalline Nanoparticles of 2, 5-Bis(4-methoxybenzylidene) Cyclopentanone. *J. Phys. Chem. B* **2008**, *112*, 2837–2841.

(9) Lau, V.; Heyne, B. Calix[4]arene Sulfonate as a Template for Forming Fluorescent Thiazole Orange H-Aggregates. *Chem. Commun.* **2010**, *46*, 3595–3597.

(10) Basak, S.; Nandi, N.; Bhattacharyya, K.; Datta, A.; Banerjee, A. Fluorescence from an H-Aggregated Naphthalenediimide Based Peptide: Photophysical and Computational Investigation of This Rare Phenomenon. *Phys. Chem. Chem. Phys.* **2015**, *17*, 30398–30403.

(11) Berlepsch, H. V.; Böttcher, C. H-Aggregates of an Indocyanine Cy5 Dye: Transition from Strong to Weak Molecular Coupling. *J. Phys. Chem. B* **2015**, *119*, 11900–11909.

(12) Mudliar, N. H.; Singh, P. K. Fluorescent H-Aggregates Hosted by a Charged Cyclodextrin Cavity. *Chem. – Eur. J.* **2016**, *22*, 7394–7398.

(13) Ryu, N.; Okazaki, Y.; Pouget, E.; Takafuji, M.; Nagaoka, S.; Ihara, H.; Oda, R. Fluorescence Emission Originated from the H-aggregated Cyanine Dye with Chiral Gemini Surfactant Assemblies Having a Narrow Absorption Band and a Remarkably Large Stokes Shift. *Chem. Commun.* **2017**, *53*, 8870–8873.

(14) Davydov, S. *Theory of Molecular Excitons*; McGraw-Hill: New York, 1962.

(15) Mishra, A.; Behera, R. K.; Behera, P. K.; Mishra, B. K.; Behera, G. B. Cyanines During the 1990s: A Review. *Chem. Rev.* **2000**, *100*, 1973–2012.

(16) von Berlepsch, H.; Böttcher, C.; Ouart, A.; Regenbrecht, M.; Akari, S.; Keiderling, U.; Schnablegger, H.; Dähne, S.; Kirstein, S. Surfactant-Induced Changes of Morphology of J-Aggregates: Superhelix-to-Tubule Transformation. *Langmuir* **2000**, *16*, 5908–5916.

(17) Struganova, I. A.; Lim, H.; Morgan, S. A. The Influence of Inorganic Salts and Bases on the Formation of the J-band in the Absorption and Fluorescence Spectra of the Diluted Aqueous Solutions of TDBC. *J. Phys. Chem. B* **2002**, *106*, 11047–11050.

(18) von Berlepsch, H.; Kristein, S.; Böttcher, C. Controlling the Helicity of Tubular J-aggregate by Chiral Alcohols. *J. Phys. Chem. B* **2003**, *107*, 9646–9654.

(19) Slavona, T. D.; Chibisov, A. K.; Görner, H. Kinetics of Salt-Induced J-aggregation of Cyanine Dyes. *J. Phys. Chem. A* **2005**, *109*, 4758–4765.

(20) Birkan, B.; Gulen, D.; Özcelik, S. Controlled Formation of the Two-Dimensional TTBC J-Aggregates in Aqueous Solution. *J. Phys. Chem. B* **2006**, *110*, 10805–10813.

(21) Yao, H.; Isohashi, T.; Kimura, K. Electrolyte-Induced Mesoscopic Aggregation of Thiacarbocyanine Dye in Aqueous Solution: Counterion Size Specificity. *J. Phys. Chem. B* **2007**, *111*, 7176–7183.

(22) von Berlepsch, H.; Kristein, S.; Hania, R.; Pugzlys, A.; Böttcher, C. Modification of the Nanoscale Structure of the J-aggregate of a Sulfonate-Substituted Amphiphilic Carbocyanine Dye through incorporation of Surfactant-Active additives. *J. Phys. Chem. B* **2007**, *111*, 1701–1711.

(23) Guralchuk, G. Y.; Katrunov, I. K.; Grynyov, R. S.; Sorokin, A. V.; Yefimova, S. L.; Borovoy, I. A.; Malyukin, Y. V. Anomalous Surfactant-Induced Enhancement of Luminescence Quantum Yield of Cyanine Dye J-Aggregates. *J. Phys. Chem. C* **2008**, *112*, 14762–14768.

(24) Kumar, V.; Baker, G. A.; Pandey, S. Ionic Liquid-Controlled J- versus H-Aggregation of Cyanine Dyes. *Chem. Commun.* **2011**, *47*, 4730–4732.

(25) Eisele, D. M.; Arias, D. H.; Fu, X.; Bloemsma, E. A.; Steiner, C. P.; Jensen, R. A.; Rebentrost, P.; Eisele, H.; Tokmakoff, A.; Lloyd, S.; et al. Robust Excitons Inhabit Soft Supramolecular Nanotubes. *Proc. Natl. Acad. Sci. U. S. A.* **2014**, *111*, E3367–E3375.

(26) Rhodes, S.; Liang, W.; Shteinberg, E.; Fang, J. Formation of Spherulitic J-Aggregates from the Coassembly of Lithocholic Acid and Cyanine Dye. *J. Phys. Chem. Lett.* **2017**, *8*, 4504–4509.

(27) Rhodes, S.; Liang, W.; Wang, X.; Reddy, N. R.; Fang, J. Transition from H-Aggregate Nanotubes to J-Aggregate Nanoribbons. *J. Phys. Chem. C* **2020**, *124*, 11722–11729.

(28) Zhang, X.; Bera, T.; Liang, W.; Fang, J. Longitudinal Zipping/Unzipping of Self-Assembled Organic Tubes. *J. Phys. Chem. B* **2011**, *115*, 14445–14449.

(29) Tellini, V. H. S.; Jover, A.; Meijide, F.; Tato, J. V.; Galantini, L.; Pavel, N. V. Supramolecular Structures Generated by a p-tert-Butylphenyl-amide Derivative of Cholic Acid: From Vesicles to Molecular Tubes. *Adv. Mater.* **2007**, *19*, 1752–1756.

(30) Selinger, J. V.; Spector, M. S.; Schnur, J. M. Theory of Self-Assembled Tubules and Helical Ribbons. *J. Phys. Chem. B* **2001**, *105*, 7157–7169.

(31) Giulieri, F.; Krafft, M. P. Tubular microstructures made from nonchiral single-chain fluorinated amphiphiles: Impact of the structure of the hydrophobic chain on the rolling-up of bilayer membrane. *J. Colloid Interface Sci.* **2003**, *258*, 335–344.

(32) Tkacheva, T. N.; Yefimova, S. L.; Klochkov, V. K.; Borovoy, I. A.; Malyukin, Y. V. Spectroscopic Study of Ordered Hybrid Complexes Formation between Dye Aggregates and ReVO4:Eu3+(Re = Y, Gd, La) Nanoparticles. *J. Mol. Liq.* **2014**, *199*, 244–250.

(33) Reddy, N. R.; Rhodes, S.; Ma, Y.; Fang, J. *Davydov Split Aggregates of Cyanine Dyes* on Self-Assembled Nanotubes. *Langmuir* **2020**, *36*, 13649–13655.

(34) Das, S.; Kamat, P. V. Can H-Aggregates Serve as Light-Harvesting Antennae? Triplet–Triplet Energy Transfer between Excited Aggregates and Monomer Thionine in Aersol-OT Solutions. *J. Phys. Chem. B* **1999**, *103*, 209–215.

(35) Minarik, W. G.; Nadeau, J. L. Photophysics of Dopamine-Modified Quantum Dots and Effects on Biological Systems. *Nat. Mater.* **2006**, *5*, 409−417.

(36) Ji, X.; Palui, G.; Avellini, T.; Na, H. B.; Yi, C.; Knappenberger, K. L., Jr.; Mattoussi, H. On the pH-Dependent Quenching of Quantum Dot Photoluminescence by Redox Active Dopamine. *J. Am. Chem. Soc.* **2012**, *134*, 6006−6017.

(37) Reddy, N. R.; Rhodes, S.; Fang, J. Colorimetric Detection of Dopamine with J-Aggregate Nanotube-Integrated Hydrogel Thin Films. *ACS Omega* **2020**, *5*, 18198−18204.

(38) Deng, J.; Liang, W.; Fang, J. Liquid Crystal Droplet Embedded Biopolymer Hydrogel Sheets for Biosensor Applications. *ACS Appl. Mater. Interfaces* **2016**, *8*, 3928−3932.

(39) Zhang, X.; Chen, X.; Kai, S.; Wang, H.-Y.; Yang, J.; Wu, F.-G.; Chen, Z. Highly Sensitive and Selective Detection of Dopamine using One-Pot Synthesized Highly Photoluminescent Silicon Nanoparticles. *Anal. Chem.* **2015**, *87*, 3360−3365.